



## NRC Publications Archive Archives des publications du CNRC

### **Structure and interactions in the anomalous swelling regime of phospholipid bilayers**

Pabst, Georg; Katsaras, John; Raghunathan, Velayudhan A.; Rappolt, Michael

This publication could be one of several versions: author's original, accepted manuscript or the publisher's version. / La version de cette publication peut être l'une des suivantes : la version prépublication de l'auteur, la version acceptée du manuscrit ou la version de l'éditeur.

For the publisher's version, please access the DOI link below. / Pour consulter la version de l'éditeur, utilisez le lien DOI ci-dessous.

<https://doi.org/10.1021/la026052e>

### **NRC Publications Record / Notice d'Archives des publications de CNRC:**

<https://nrc-publications.canada.ca/eng/view/object/?id=f250b478-5ff0-4b72-8aa4-47a3c768b495>

<https://publications-cnrc.canada.ca/fra/voir/objet/?id=f250b478-5ff0-4b72-8aa4-47a3c768b495>

Access and use of this website and the material on it are subject to the Terms and Conditions set forth at

<https://nrc-publications.canada.ca/eng/copyright>

READ THESE TERMS AND CONDITIONS CAREFULLY BEFORE USING THIS WEBSITE.

L'accès à ce site Web et l'utilisation de son contenu sont assujettis aux conditions présentées dans le site

<https://publications-cnrc.canada.ca/fra/droits>

LISEZ CES CONDITIONS ATTENTIVEMENT AVANT D'UTILISER CE SITE WEB.

**Questions?** Contact the NRC Publications Archive team at

PublicationsArchive-ArchivesPublications@nrc-cnrc.gc.ca. If you wish to email the authors directly, please see the first page of the publication for their contact information.

**Vous avez des questions?** Nous pouvons vous aider. Pour communiquer directement avec un auteur, consultez la première page de la revue dans laquelle son article a été publié afin de trouver ses coordonnées. Si vous n'arrivez pas à les repérer, communiquez avec nous à PublicationsArchive-ArchivesPublications@nrc-cnrc.gc.ca.



# Structure and Interactions in the Anomalous Swelling Regime of Phospholipid Bilayers<sup>†</sup>

Georg Pabst,<sup>‡,§</sup> John Katsaras,<sup>\*,‡</sup> Velayudhan A. Raghunathan,<sup>||</sup> and Michael Rappolt<sup>§</sup>

National Research Council, Steacie Institute for Molecular Sciences, Bldg. 459, Stn. 18, Chalk River, Ontario, K0J 1J0, Canada, Institute of Biophysics and X-Ray Structure Research, Austrian Academy of Sciences, Schmiedlstrasse 6, 8042 Graz, Austria, and Raman Research Institute, Bangalore 560 080, India

Received June 10, 2002. In Final Form: October 16, 2002

We have carried out X-ray and neutron diffraction experiments, as a function of temperature, on fully hydrated samples of dimyristoyl phosphatidylcholine bilayers. The data show the following: (a) In the vicinity of the  $L_{\alpha}$  to  $P_{\beta}$  transition, we find an anomalous expansion of the water layer of  $\sim 1.7$  Å. (b) The lipid bilayer thickness increases quasi-linearly and is similar to the increase in the lamellar repeat spacing  $d$  found in dimyristoyl ethanolamine bilayers in the temperature range of  $T_M$  to  $T_M + 13$  °C. (c) In contrast to an earlier study, we find no significant changes to the steric size of the phosphatidylcholine headgroup. The anomalous increase in  $d$  is thus dominated by an expansion of the water layer. This expansion is caused by a distinct increase in bilayer fluctuations as revealed by an analysis of the Caillé parameter. Additional osmotic pressure experiments not only support this notion but have allowed us to further estimate the temperature dependence of both the bilayer bending rigidity,  $K_c$ , and the interbilayer compressional parameter,  $B$ . Both  $K_c$  and  $B$  experience an abrupt decrease on approaching  $T_M$  from above, indicative of a “softening” of the bilayers.

## 1. Introduction

Among the many supramolecular structures displayed by phospholipid/water systems,<sup>1</sup> the liquid-crystalline,  $L_{\alpha}$ , phase is considered to be biologically relevant. As a result, many efforts have been undertaken in order to better understand both the structural and mechanical properties of this phase.<sup>2</sup> Another major focus in the area of model membranes involves phase transition phenomena, especially in the vicinity of the  $L_{\alpha}$  phase, as it is believed that certain physiologically processes may be dependent on membrane gelation.<sup>3</sup> For example, it has been suggested recently that the proximity of membranes to the gel state is of principal importance for certain processes occurring in the brain, the physiology of thermoregulation, and mechanisms of general anesthesia.<sup>4</sup>

In the case of multibilayer stacks of dimyristoyl phosphatidylcholine (DMPC), one particularly intriguing phase transition involves the structural changes close to the main transition ( $L_{\alpha} \rightarrow P_{\beta}$ ) temperature,  $T_M$ . With decreasing temperature, fluidlike,  $L_{\alpha}$  DMPC bilayers exhibit a nonlinear increase in their lamellar repeat spacing,  $d$  (Figure 1), which has previously been reported by various groups for DMPC and other lipid/water systems.<sup>5–14</sup>

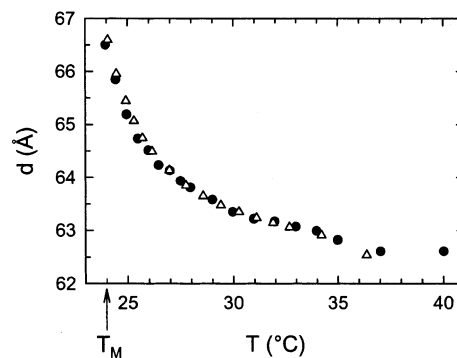


**Figure 1.** Anomalous swelling of  $L_{\alpha}$  DMPC bilayer stacks as a function of decreasing temperature ( $T_M = 24.0$  °C). The ●'s correspond to X-ray diffraction data of liposomal preparations, while the Δ's are the result of neutron diffraction studies on aligned systems.

Presently, the accepted view is that this anomalous swelling is a pretransitional effect. This may be the result of either a critical transition being intercepted by a first-order main transition<sup>15</sup> or the fact that the main transition is weakly first order due to some intrinsic properties of the bilayer.<sup>16</sup> Furthermore, there are a number of other

\* To whom correspondence should be addressed. Tel: 613-584-8811 ext 3984. Fax: 613-584-4040. E-mail: John.Katsaras@nrc.ca.

<sup>†</sup> Part of the *Langmuir* special issue entitled The Biomolecular Interface.

<sup>‡</sup> Steacie Institute for Molecular Sciences.

<sup>§</sup> Austrian Academy of Sciences.

<sup>||</sup> Raman Research Institute.

(1) See, for example: Seddon, J. M.; Templer, R. H. In *Structure and Dynamics of Membranes*; Lipowsky, R., Sackmann, E., Eds.; North-Holland: Amsterdam, 1995; p 97.

(2) Nagle, J. F.; Tristram-Nagle, S. *Biochim. Biophys. Acta* **2000**, *1469*, 159.

(3) Melchior, D. L.; Steim, J. M. *Annu. Rev. Biophys. Bioeng.* **1976**, *5*, 205. Hazel, J. R. *Annu. Rev. Physiol.* **1995**, *57*, 19.

(4) Kharakoz, D. *Biophysics* **2000**, *45*, 554.

(5) Kirchner, S.; Cevc, G. *Europhys. Lett.* **1993**, *23*, 229.

(6) Hønger, T.; Mortensen, K.; Ipsen, J. H.; Lemmich, J.; Bauer, R.; Mouritsen, O. G. *Phys. Rev. Lett.* **1994**, *72*, 3911.

(7) Zhang, R.; Sun, W.; Tristram-Nagle, S.; Headrick, R. L.; Suter, R. M.; Nagle, J. F. *Phys. Rev. Lett.* **1995**, *74*, 2832.

(8) Lemmich, J.; Mortensen, K.; Ipsen, J. H.; Hønger, T.; Bauer, R.; Mouritsen, O. G. *Phys. Rev. Lett.* **1995**, *75*, 3958.

(9) Chen, F. Y.; Hung, W. C.; Huang, H. W. *Phys. Rev. Lett.* **1997**, *79*, 4026.

(10) Nagle, J. F.; Petrache, H. I.; Gouliev, N.; Tristram-Nagle, S.; Liu, Y.; Suter, R. M.; Gawrisch, K. *Phys. Rev. E* **1998**, *58*, 7769.

(11) Richter, F.; Finegold, L.; Rapp, G. *Phys. Rev. E* **1999**, *59*, 3483.

(12) Korreman, S. S.; Posselt, D. *Eur. Phys. J.* **2000**, *1*, 87.

(13) Mason, P. C.; Nagle, J. F.; Eppard, R. M.; Katsaras, J. *Phys. Rev. E* **2001**, *63*, 030902–1.

(14) Korreman, S. S.; Posselt, D. *Eur. Biophys. J.* **2001**, *30*, 121.

(15) Nagle, J. F. *Proc. Natl. Acad. Sci. U.S.A.* **1973**, *70*, 3443.

quantities (e.g., passive bilayer permeability, heat capacity, fluorescence lifetime of *trans*-parinaric acid in bilayers, NMR order parameter, and ultrasound velocity) which exhibit anomalous behavior near  $T_M$ .<sup>17</sup> Nevertheless, the fact that similar transition enthalpies, including the dependence on the hydrocarbon chain length, have been observed in lipid systems which exhibit no pretransitional swelling<sup>18</sup> suggests that parts of the theory need to be revised.

Despite many efforts, a complete picture of the structural changes in the anomalous swelling regime is presently still lacking. Commonly reported structural parameters are lipid bilayer thickness,  $d_B$ , and the thickness of the water layer  $d_W$ . The sum of these parameters gives rise to the lamellar periodicity,  $d$ .  $d_B$  can be further subdivided as  $2d_H + 2d_C$  where  $d_H$  is the steric size of the polar phosphorylcholine headgroup and  $d_C$  is the effective length of the hydrophobic fatty acid chains. Over the years, various and sometimes conflicting views on which of these structural components accounts for most or all of the observed anomalous swelling have been reported in the literature.<sup>6–10</sup>

In the mid-1990s, the Danish group of Mouritsen<sup>6,8</sup> attributed the anomalous swelling to the thickening of the hydrophilic layer, which they defined as the sum of  $d_W$  and  $2d_H$ . Moreover, they mentioned that this increase was due to increased bilayer fluctuations. This notion was supported by an earlier study which found a decrease in the membrane bending rigidity using shape analysis on giant unilamellar vesicles.<sup>19</sup> However, Nagle et al.<sup>10</sup> noted that the decrease in the membrane bending rigidity may have been the result of Fernandez-Puente et al. assuming a constant vesicular volume in their data analysis. Later on, Huang and co-workers performed experiments on partially hydrated aligned systems of dilauroyl phosphatidylcholine (DLPC) bilayers,<sup>9</sup> which lent further support to the conclusions espoused by Mouritsen and co-workers.<sup>6,8</sup> However, their extrapolation to fully hydrated conditions yielded a  $d$  which was  $\sim 5 \text{ \AA}$  less than what is commonly measured in fully hydrated DLPC bilayers.<sup>20</sup>

In response to the first paper by Mouritsen and co-workers,<sup>6</sup> Nagle's group, at Carnegie Mellon, performed line-shape analysis on high-resolution X-ray data using the modified Caillé theory (MCT)<sup>21</sup> and suggested that the anomalous change in  $d$  near  $T_M$  could almost entirely be attributed to an increase in the thickness of the hydrophobic part,  $2d_C$ , of the bilayer.<sup>7</sup> In 1998, Nagle et al. extended their model by stating that  $2d_C$  does indeed swell<sup>10</sup> but scaling of this contribution to  $d$  left an anomalous component of  $\sim 2 \text{ \AA}$ , unexplained. This notion of the unexplained  $2 \text{ \AA}$  of anomalous swelling was further confirmed by Mason et al.,<sup>22</sup> using a DMPC sample of large unilamellar vesicles (LUVs). Assuming that the unaccounted  $2 \text{ \AA}$  is due to an expansion of the water layer,

Nagle et al. performed Monte Carlo simulations.<sup>10</sup> For this scenario, the simulations predicted a 35% increase in the Caillé parameter, which is a measure of the thermal undulations of the bilayers, in the vicinity of  $T_M$ . However, analysis of the experimental data did not show an increase in bilayer fluctuations and was consistent with additional osmotic pressure experiments.

In the aftermath of the above-mentioned studies, additional models were advanced. One such model speculates that the water spacing could expand because of changes in either the repulsive hydration force or the attractive van der Waals force in the vicinity of  $T_M$ .<sup>10</sup> However, quantitative support for this scenario has yet to be found. Another model proposes that the headgroup region can swell anomalously, thus accounting for the elusive  $2 \text{ \AA}$ .<sup>10</sup> However, NMR data suggested a maximum headgroup contribution of  $0.6 \text{ \AA}$ .<sup>10</sup>

In this paper, we report X-ray and neutron diffraction studies, as a function of temperature, on fully hydrated liposomal preparations and highly aligned multibilayers of DMPC. The powder data were analyzed using the recently developed full  $q$  refinement method.<sup>23</sup> In the vicinity of the  $L_\alpha \rightarrow P_\beta$  transition, we find that the water layer,  $d_W$ , experiences a sudden expansion of about  $1.7 \text{ \AA}$ . On the other hand, the hydrophobic bilayer thickness also increases but does not contribute to an anomalous increase in  $d$ , since its trend for  $d$  is similar to that observed in dimyristoyl ethanolamine (DMPE) whose main transition is not considered as being "anomalous".<sup>13</sup> We further find no significant contribution to anomalous swelling of the hydrophilic phosphatidylcholine headgroup. An analysis of the undulation parameter revealed increased bilayer fluctuations on approaching  $T_M$ , consistent with the expansion of the water layer. The increased bilayer fluctuations can be explained by a reduced bilayer bending rigidity,  $K_c$ , and a decrease in the interbilayer compressibility,  $B$ . Osmotic pressure experiments on the aligned samples support our results of the fluctuation analysis. Moreover, we were able to estimate the temperature dependence of both  $K_c$  and  $B$ . Our estimates indicate that  $K_c$  reduces by 20% near  $T_M$ , while the reduction in  $B$  is  $\sim 12\%$ . These observations account for all of the outstanding issues concerning structure and interactions in the anomalous swelling regime of DMPC bilayers and possibly of all lipid bilayers exhibiting similar behavior.

## 2. Materials and Experimental Methods

**2.1. Sample Preparation.** DMPC was purchased from Avanti Polar Lipids (Birmingham, AL) and used without further purification. Poly(*n*-vinylpyrrolidone) (PVP) of average molecular weight 40 000 was purchased from Sigma Chemical Co. (Milwaukee, WI), and  $D_2O$  of 99.92 wt % purity from Atomic Energy of Canada Ltd. (Chalk River, ON).

Multilamellar liposomes were prepared in the following manner: DMPC was dissolved in a solvent of  $CHCl_3/CH_3OH$  (2:1, v/v). The solution was then dried under a stream of  $N_2$  gas and subsequently placed under vacuum for a period of 12 h. The desiccated lipid was then hydrated using double-distilled/deionized water yielding samples containing 25 wt % lipid. To ensure complete hydration, the lipid dispersions were incubated for 30 min at  $60 \text{ }^\circ\text{C}$  ( $36 \text{ }^\circ\text{C}$  above the main transition). The liposomal preparations were further annealed in the following manner: (a) 2 min of vigorous vortexing, (b) 5 min of equilibration at  $10 \text{ }^\circ\text{C}$ , and (c) a further 5 min of equilibration at  $60 \text{ }^\circ\text{C}$ . Steps a–c were repeated a total of five times. When this method of liposomal preparation is used, the samples display a narrow, cooperative melting transition. Thin-layer chromatography was carried out on all samples before and after experimentation.

(16) Kharakoz, D. P.; Shlyapnikova, E. A. *J. Phys. Chem. B* **2000**, *104*, 10368.

(17) Nagle, J. F.; Scott, H. L. *Biochim. Biophys. Acta* **1978**, *513*, 236. Hatta, I.; Suzuki, K.; Imaizumi, S. *J. Phys. Soc. Jpn.* **1983**, *52*, 2790. Rugerio, A.; Hudson, B. *Biophys. J.* **1989**, *55*, 1111. Morrow, M. R.; Whitehead, J. P.; Lu, D. *Biophys. J.* **1992**, *63*, 18. Kharakoz, D. P.; Colloto, A.; Lohner, K.; Laggner, P. *J. Phys. Chem.* **1993**, *97*, 9844.

(18) Koyova, R.; Caffrey, M. *Chem. Phys. Lipids* **1994**, *69*, 1. Koyova, R.; Caffrey, M. *Biochim. Biophys. Acta* **1998**, *1376*, 91.

(19) Fernandez-Puente, L.; Bivas, I.; Mitov, M. D.; Méléard, P. *Europhys. Lett.* **1994**, *28*, 181.

(20) Hatta, I.; Matuoka, S.; Singer, M. A.; Finegold, L. *Chem. Phys. Lipids* **1994**, *69*, 129.

(21) Zhang, R.; Suter, R. M.; Nagle, J. F. *Phys. Rev. E* **1994**, *50*, 5047.

(22) Mason, P. C.; Gaulin, B. D.; Epand, R. M.; Katsaras, J. *Phys. Rev. E* **2000**, *61*, 5634.

(23) Pabst, G.; Rappolt, M.; Amenitsch, H.; Laggner, P. *Phys. Rev. E* **2000**, *62*, 4000.



The oriented samples were prepared by first spreading a lipid solution, typically 20 mg of lipid in methanol, on a clean substrate of silicon (48 mm × 18 mm × 0.3 mm). After evaporation of the solvent, the samples were kept in a vacuum for between 12 and 24 h to remove any traces of methanol. The lipid films were subsequently annealed for 12–24 h at 70 °C in a D<sub>2</sub>O-saturated environment.

**2.2. X-ray Measurements.** X-ray diffraction patterns were recorded at the Austrian SAXS (small-angle X-ray scattering) beamline<sup>24,25</sup> (Sincrotrone Trieste, Italy). A one-dimensional position sensitive detector<sup>26</sup> was used covering a  $q$ -range ( $q = 4\pi \sin(\theta)/\lambda$ ) of between 0.03 and 0.6 Å<sup>-1</sup> at a photon energy of 8 keV. The angular calibration of the detector was performed with silver-behenate [CH<sub>3</sub>(CH<sub>2</sub>)<sub>20</sub>-COOAg] whose  $d$  corresponds to 58.38 Å.<sup>27</sup> The instrumental resolution, which was accounted for in the data analysis, was determined to have a full width at half-maximum of  $\delta q = 2.2 \times 10^{-3}$  Å<sup>-1</sup>.

X-ray measurements of the lipid dispersions were carried out with the samples placed in thin-walled, 1 mm diameter quartz capillary tubes. The capillary tubes were placed in a sample holder block of brass whose entry and exit windows were covered with a thin polymer film in order to avoid any convection induced by the surrounding environment. The temperature of the sample holder was controlled with a circulating water bath to within ±0.1 °C. The temperature was measured in the vicinity of the capillary with a Pt-100 resistance temperature detector. Prior to exposure, the sample was equilibrated for a period of 10 min for a given temperature. To prevent radiation damage, the capillaries were translated vertically by 1 mm to an unexposed portion of the sample after every second measurement. Exposure times were typically between 2 and 3 min.

**2.3. Neutron Measurements.** For the neutron scattering experiments, the substrate was mounted in an aluminum cell, described in refs 28 and 29, containing various concentrations of PVP in D<sub>2</sub>O. The PVP polymer weight concentration was converted into pressure according to McIntosh and Simon.<sup>30</sup> Osmotic pressure data were obtained at values of  $P = 0, 0.4, 2.2, 7,$  and  $16$  atm while the entire aligned sample was covered by a 6.5 mm layer of solution. The experiments were carried out at the NRU reactor, Chalk River Laboratories, using the N5 triple-axis spectrometer. Neutrons of wavelength 2.37 Å were selected using the (002) reflection of a pyrolytic-graphite monochromator. All samples were equilibrated for about 10 h before starting the measurements.

**2.4. Data Analysis.** Powder data were corrected for detector efficiency and background noise from the water and sample cell. The scattered intensity of the corrected static diffraction patterns was analyzed in terms of

$$I(q) = \frac{S(q)|F(q)|^2}{q^2} \quad (1)$$

using a MCT structure factor<sup>21,23</sup> given by

$$S(q) = N + 2 \sum_{k=1}^{N-1} (N-k) \cos(kqd) e^{-(d/2\pi)^2 q^2 \eta_1 \gamma} (\pi k)^{-(d/2\pi)^2 q^2 \eta_1} \quad (2)$$

Herein,  $N$  is the mean number of bilayers per scattering domain,  $\gamma$  is Euler's constant, and  $\eta_1$  is the fluctuation or Caillé parameter.  $\eta_1$  is related to the bilayer bending rigidity  $K_c$  and the bulk

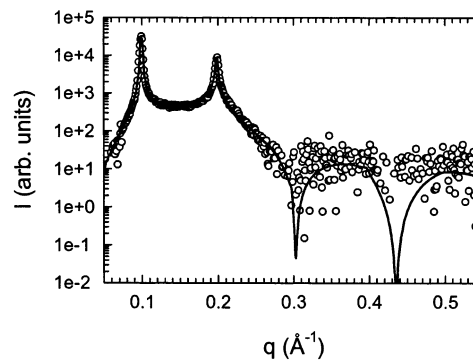


**Figure 2.** Diffraction pattern of fully hydrated DMPC multilamellar vesicles at 30 °C. In addition to the diffuse scattering, the pattern exhibits two sharp reflections corresponding to the first- and second-order quasi-Bragg peaks. The modulation of the diffuse scattering, which is best visible at higher  $q$  values, is essentially due to the bilayer form factor (see eq 1). The scattered intensity has been plotted on a logarithmic scale in order to simultaneously show both the sharp Bragg peaks and diffuse scattering. The solid line shows the best fit to the data.

**Table 1. Fit Results Applying the Full  $q$  Refinement Model to the Diffraction Data of DMPC at 30 °C<sup>a</sup>**

parameter	value	parameter	value
$\chi^2$	3.5	$d$ (Å)	$63.35 \pm 0.05$
$z_H$ (Å)	$17.34 \pm 0.06$	$\eta_1$	$0.077 \pm 0.001$
$\sigma_H$ (Å)	$3.02 \pm 0.04$	$N$	$29 \pm 1$
$\sigma_C$ (Å)	$4.46 \pm 0.13$	$k$ ( $10^{-3}$ arb. units)	$1.1 \pm 0.1$
$\bar{\rho}$	$-1.13 \pm 0.02$		

<sup>a</sup>  $k$  is the global scaling factor of the model to the scattered intensity.

modulus of compression  $B$  by<sup>31</sup>

$$\eta_1 = \frac{\pi k_B T}{2\sqrt{BK_c} d^2} \quad (3)$$

where  $K_c = Kd$ , with  $K$  corresponding to the bending modulus. The bulk modulus is a phenomenological constant in a harmonic approximation for the interaction energy between two bilayers in its discrete description.<sup>32,33</sup> It is related by  $B = B_3/d$  to the bulk modulus of the continuum description of the elasticity of smectic A liquid crystals.<sup>34</sup> The form factor

$$F(q) = \sqrt{2\pi} [2\sigma_H \exp(-\sigma_H^2 q^2/2) \cos(qz_H) + \sigma_C \bar{\rho} \exp(-\sigma_C^2 q^2/2)] \quad (4)$$

is given by the Fourier transform of the electron density profile model.<sup>23</sup> The model consists of three Gaussians representing the polar headgroups at  $\pm z_H$  and the terminal methyl groups at the center of the bilayer. The corresponding widths of the Gaussians are given by  $\sigma_H$  and  $\sigma_C$ , respectively, whereas  $\bar{\rho}$  is the fraction of the headgroup amplitude to the negative methyl terminus amplitude ( $\rho_H$  is set equal to 1). Figure 2 shows a typical fit to our data; the fit results are summarized in Table 1, while the corresponding electron density profile is presented in Figure 3.

The decomposition of the lamellar spacing,  $d$ , into  $d_W$  and  $d_B$  is not trivial, the reason being that the electron density profiles which can be reconstructed from the diffraction patterns are of low resolution (Figure 3). In some sense, we can exploit this in our favor because we can use the simple Gaussian model described above to represent the electron density to a good approximation. Nevertheless, how does one distinguish between  $d_W$  and  $d_B$ ? A

(24) Amenitsch, H.; Bernstorff, S.; Rappolt, M.; Kriechbaum, M.; Mio, H.; Laggner, P. *J. Synchrotron Rad.* **1998**, *5*, 506.

(25) Bernstorff, S.; Amenitsch, H.; Laggner, P. *J. Synchrotron Radiat.* **1998**, *5*, 1215.

(26) Petrascu, A.-M.; Koch, M. H. J.; Gabriel, A. *J. Macromol. Sci., Phys.* **1998**, *37*, 463.

(27) Huang, T. C.; Toraya, H.; Blanton, T. N.; Wu, Y. *J. Appl. Crystallogr.* **1993**, *26*, 180.

(28) Katsaras, J. *Biophys. J.* **1998**, *75*, 2157.

(29) Pabst, G.; Katsaras, J.; Raghunathan, V. A. *Phys. Rev. Lett.* **2002**, *88*, 128101.

(30) McIntosh, T. J.; Simon, S. A. *Biochemistry* **1986**, *25*, 4058.

(31) Caillé, A. C. R. *Seances Acad. Sci., Ser. B* **1972**, *274*, 891.

(32) Holyst, R. *Phys. Rev. A* **1991**, *44*, 3692. Lei, N.; Safinya, C. R.; Bruinsma, R. F. *J. Phys. II* **1995**, *5*, 1155.

(33) Petrache, H. I.; Gouliaev, N.; Tristram-Nagle, S.; Zhang, R.; Suter, R. M.; Nagle, J. F. *Phys. Rev. E* **1998**, *57*, 7014.

(34) DeGennes, P. G. *J. Phys. (Paris), Colloq.* **1969**, *30*, C4–65.

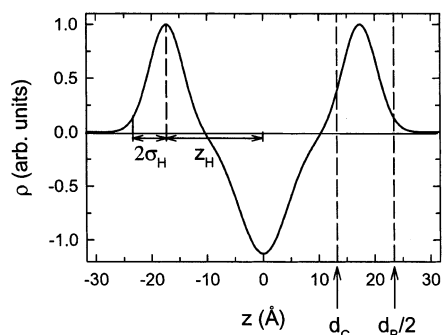


**Figure 3.** Electron density profile model, represented by the summation of three Gaussians. The Gaussians centered at  $\pm z_H$  characterize the headgroup, and their  $2\sigma_H$  width toward the water layer defines the boundary of the bilayer. The boundary of the hydrocarbon region,  $2d_C$ , is calculated using parameters from the gel phase.

recent review by Nagle and Tristram-Nagle<sup>2</sup> deals with this difficulty. In this paper, we are more interested in the temperature dependence of  $d_W$  and  $d_B$ ; as such, it is not of outmost importance to know the absolute values of these two parameters. Thus, we obtain the bilayer thickness from the electron density profiles in the following manner:

$$d_B = 2(z_H + 2\sigma_H) \quad (5)$$

This is a definition that has previously been used for  $L_{\beta}$  bilayers.<sup>35</sup> The use of eq 5 is further motivated by Figure 2 of ref 2. Since X-rays are most sensitive to the electron-rich phosphate ( $\text{PO}_4$ ) fragment of the headgroup and are practically insensitive to the choline group, the headgroup Gaussian represents, mainly, the  $\text{PO}_4$  component. Figure 2 of ref 2 shows the electron density profile of fully hydrated dipalmitoyl phosphatidylcholine (DPPC) together with probability distributions for different component groups from simulations. According to this figure,  $z_H + 2\sigma_H$  cuts the probability distribution of the choline group near its half value and may therefore be seen as a Gibbs dividing surface for the bilayer.<sup>36</sup>

The lateral area,  $A$ , per lipid is calculated according to<sup>2</sup>

$$A = (V_L - V_H)/d_C \quad (6)$$

where  $V_L$  is the lipid volume and  $V_H$  is the volume of the headgroup.  $V_L$  is obtained from volumetric measurements; for the present data, we have used the results for DMPC reported by Laggner and Stabinger.<sup>37</sup> For phosphorylcholine headgroups,  $V_H$  is equal to 319 Å.<sup>32</sup> The effective hydrocarbon chain length

$$d_C = d_B/2 - d_H \quad (7)$$

is obtained by constraining  $d_C$  to give the best overall agreement to the  $d_C$  obtained from NMR measurements<sup>10</sup> (see section III).

A different approach, referred to as the “bootstrap method”, derives  $d_C$  from

$$d_C = z_H - d_{H1} \quad (8)$$

where  $d_{H1}$  is the distance from the  $\text{PO}_4$  group to the boundary between the polar and the lipophilic region of the bilayer.<sup>2</sup> Nagle and co-workers usually use a  $d_{H1}$  of 4.1 Å;<sup>2</sup> however, Balgavý et al.<sup>38</sup> have found, from small-angle scattering experiments on LUVs, that this value varies with the hydrocarbon chain length. Further, different definitions of the electron density model may

(35) Wiener, M. C.; Suter, R. M.; Nagle, J. F. *Biophys. J.* **1989**, *55*, 315.

(36) Parsegian, V. A.; Rand, P. In *Structure and Dynamics of Membranes*; Lipowsky, R., Sackmann, E., Eds.; North-Holland: Amsterdam, 1995; p 643.

(37) Laggner, P.; Stabinger, H. In *Colloid and Interface Science*; Kerker, M., Ed.; Academic Press: New York, 1976; Vol. 5, p 91.

(38) Balgavý, P.; Dubnicková, M.; Kučerka, N.; Kiselev, M. A.; Yaradaikin, S. P.; Uhríková, D. *Biochim. Biophys. Acta* **2001**, *1512*, 40.

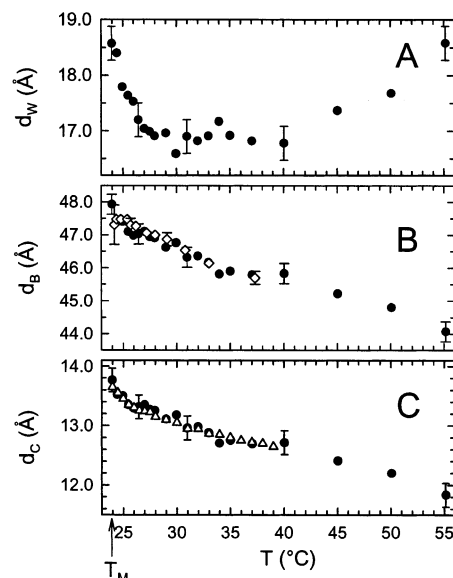


**Figure 4.** Temperature dependence of the water layer thickness  $d_W$ , bilayer thickness  $d_B$ , and effective hydrocarbon chain length  $d_C$  in fully hydrated DMPC. The  $\diamond$ 's in panel B correspond to the  $d$  values in DMPE (ref 13) scaled in temperature by subtracting 25 °C and in  $d$  by subtracting 2.8 Å. The  $\triangle$ 's in the  $d_C(T)$  plot correspond to NMR measurements on DMPC-d54 (ref 10) and are shifted in temperature by 4 °C.

**Table 2. Comparison of Structural Parameters from Present Data to Those by Nagle and Co-workers (Reference 2) for DMPC Bilayers at 30 °C<sup>a</sup>**

parameter	present	ref 2	parameter	present	ref 2
$d$ (Å)	63.4	62.7	$d_C$ (Å)	13.2	13.1
$d_B$ (Å)	46.8	44.2	$A$ (Å <sup>2</sup> )	59.4	59.1
$d_W$ (Å)	16.6	18.5			

<sup>a</sup> The definition of  $d_B$  differs in the two studies (see data analysis).

lead to slightly different  $z_H$  values. This results in an additional variation of  $d_{H1}$ , which in total is assumed to be between 4.1 and 5.5 Å.<sup>38</sup> Though these are details important in determining the absolute parameter values, they are not a severe restriction to the present study as we are more interested in their relative changes as a function of temperature. Nevertheless, we note that using a  $d_{H1}$  of 4.1 Å gives good agreement between our  $d_C$  and the corresponding values obtained from NMR<sup>10</sup> and X-ray diffraction studies<sup>2</sup> (see below).

The above method further obtains the membrane thickness from eqs 7 and 8 by adding a steric headgroup size of 9 Å (ref 2) or 10 Å (ref 40). This is different from our definition of  $d_B$  (eq 5). However, the headgroup was implicated in taking part in anomalous swelling.<sup>10</sup> Therefore, we need to have  $d_H$  freely adjustable and not fixed to a predetermined value. This is the primary reason we chose eq 5 to calculate  $d_B$  and require that the  $d_C$  values be in good agreement with the NMR data. Compared to the bootstrap method (eq 7), the differences in the  $d_C$  values are minor. However, as will become clear in the following section, with the present method we get a more robust estimate for  $d_H$ .

### 3. Results and Discussion

**3.1. Structural Parameters.** The structural results of the full  $q$  refinement method are summarized in Figure 4. Table 2 presents a comparison between the present results and those of Nagle and co-workers<sup>10</sup> at 30 °C. Starting at 55 °C and on decreasing temperature, we observe that  $d_W$  first decreases and then begins to level off at  $\sim 40$  °C (Figure 4a). At high temperatures, the

(39) Pabst, G.; Rappolt, M.; Amenitsch, H.; Bernstorff, S.; Laggner, P. *Langmuir* **2000**, *16*, 8994.

(40) McIntosh, T. J.; Simon, S. A. *Biochemistry* **1986**, *25*, 4948.

increase of  $d_w$  is the result of increased fluctuations (see also Figure 6) and has been described in detail elsewhere.<sup>10,29,39</sup> Here, we concentrate on the structural changes close to  $T_M$ , where the water layer starts, at around 27 °C, to expand abruptly. Just before  $T_M$ , the nonlinear expansion of  $d_w$  amounts to about 1.7 Å (Figure 4a). The bilayer, on the other hand, shows a continuous increase in thickness as the temperature is lowered (Figure 4b). This is consistent with the picture of “freezing out” the conformational disorder of the hydrocarbon chains on approaching the main transition. The hydrocarbon chain length (Figure 4c) has been obtained, as described in the previous section, and resulted in a  $d_H$  value of 10.2 Å. For comparison, Figure 4c also contains the data from NMR measurements<sup>10</sup> used to obtain our  $d_C$ .  $T_M$  for DMPC-d54 is  $\sim 20.0$  °C. Assuming this to be the only difference between the two systems, we shifted the NMR data upward by 4 °C. Both data show a good overall agreement using a single fixed  $d_H$ . It is gratifying to note that our estimate for  $d_H$  is similar to that reported in the literature.<sup>40,41</sup>

We have further calculated  $d_C$  according to eq 8 and derived  $d_H$  using eq 7. This method yields values of  $d_H$  between 10.0 and 10.2 Å. Such variations are smaller than the error in determining  $d_H$ , and this further justifies our decision to keep  $d_H$  at the single fixed value mentioned previously. Consequently, we infer that  $d_H$  does not contribute to anomalous swelling. Recently, Fragneto et al. reported neutron reflectivity studies on a novel system consisting of only two bilayers, one of which is adsorbed on a solid support.<sup>42</sup> Such a system of distearoyl phosphatidylcholine (DSPC) exhibited a large water layer thickness of about 60 Å close to  $T_M$ , which decreased to  $\sim 20$  Å at higher temperatures. This result by Fragneto et al. is in good agreement with our observations for  $d_w$ . More importantly, they found no significant changes to  $d_H$ .<sup>42</sup>

A clear definition of what constitutes anomalous swelling has been elusive. Most of the earlier reports defined the nonlinear behavior of  $d$  as anomalous swelling.<sup>7,9–14</sup> However,  $d$  also shows a strong temperature dependence at higher temperatures.<sup>29</sup> Here, we take the observed increase of  $d$  in DMPE on approaching  $T_M$  as the “normal” trend and any amount of swelling over and above this trend as being anomalous.<sup>13</sup> Further, the increase in  $d$  for DMPE<sup>13</sup> is strikingly similar to the increase of  $d_B$  (Figure 4b). Both show an almost linear increase of 1.5–2.0 Å in the temperature range of  $T_M$  to  $T_M + 13$  °C. Thus, the anomalous increase in  $d$  for DMPC multibilayer stacks is essentially due to an expansion of the water layer.

Why then does the water layer expand anomalously? As discussed by Nagle et al.,<sup>10</sup> one possibility is that there is a change in the hydration force due to a decrease in lateral area per lipid. This would mean that the bilayer surface becomes “gel-like” close to  $T_M$ . Measurements by McIntosh and Simon indicate that the hydration force is increased in the gel phase.<sup>43</sup> However, as noted by Nagle et al. the hydration force is not dominant in the case of fully hydrated bilayers.<sup>10</sup> Long-range interactions are governed by attractive van der Waals and repulsive steric interactions arising from undulations. Here we show the temperature dependence of the lateral area per lipid molecule (Figure 5). The area decreases linearly from 66.8 Å<sup>2</sup> at 55 °C to 58.0 Å<sup>2</sup> at 25.5 °C and then experiences a

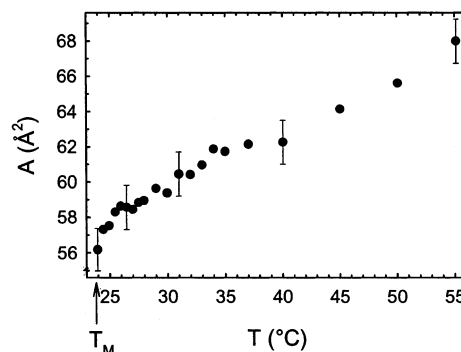


**Figure 5.** The lateral area per lipid as a function of temperature of fully hydrated DMPC bilayers.

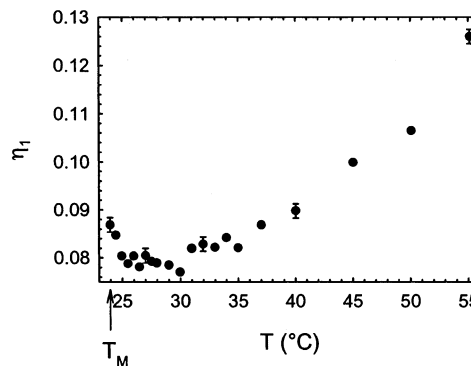


**Figure 6.** The Caillé or fluctuation parameter  $\eta_1$  as a function of temperature for fully hydrated DMPC bilayers.  $\eta_1$  was obtained by a global fit of the X-ray diffraction pattern.

sudden drop, to 56.2 Å<sup>2</sup>, in the vicinity of  $T_M$ . The total fractional decrease of  $A$ , within the temperature range of  $T_M$  to  $T_M + 10$  °C,<sup>44</sup> is about 8%. However,  $A$  in gel-phase bilayers is about 0.24 times smaller than in the  $L_\alpha$  phase.<sup>2</sup> Thus, the observed decrease in  $A$  is insufficient to explain a gel-phase-like hydration force interaction.

Another possibility then, is that the van der Waals attraction force between bilayers is altered, though this has also been excluded by Nagle et al.,<sup>10</sup> since the observed increase in  $d_B$  results in an increase of this attraction. This would then favor decreasing, rather than increasing,  $d_w$ . They further remarked that effects on the Hamaker constant can be neglected.

**3.2. Fluctuation Analysis.** In this last section, we come to the conclusion that the anomalous expansion of  $d_w$  cannot be attributed to changes in either the hydration or the van der Waals force. On the other hand, bilayer fluctuations, inherent to the  $L_\alpha$  phase, lead to an effective long-range repulsive interaction of entropic origin.<sup>45</sup> Moreover, fluctuations are known to affect the shape of the lamellar scattering peaks;<sup>31</sup> in particular, the long power law tails seen in Bragg peaks are governed by the Caillé parameter  $\eta_1$

$$I(q - q_h) \propto (q - q_h)^{-(1-\eta_h)} \quad (9)$$

where  $h$  gives the diffraction order and  $\eta_h \approx \eta_1 h^2$ .<sup>31</sup> The MCT structure factor (eq 2) accounts for these changes in the line shape of the diffraction orders, opening an experimental window on fluctuations. Figure 6 shows our results for the temperature dependence of  $\eta_1$ .

(41) Büldt, G.; Gally, H. U.; Seelig, J.; Zaccai, G. *J. Mol. Biol.* **1979**, *134*, 673. Zaccai, G.; Büldt, G.; Seelig, A.; Seelig, J. *J. Mol. Biol.* **1979**, *134*, 693.

(42) Fragneto, G.; Charitat, T.; Graner, F.; Mecke, K.; Perino-Gallice, L.; Bellet-Amalric, E. *Europhys. Lett.* **2001**, *53*, 100.

(43) McIntosh, T. J.; Simon, S. A. *Biochemistry* **1993**, *32*, 8374.

(44)  $T_M + 10$  °C is outside the anomalous regime (Figure 1), where no effects of an increased bilayer density are observed.

(45) Helfrich, W. *Z. Naturforsch., A* **1978**, *33a*, 305.



Starting at  $T_M$ ,  $\eta_1$  rapidly decreases by about 10% and then remains constant up to a temperature of about 30 °C. At higher temperatures,  $\eta_1$  again experiences an increase of ~60%. This increase at high temperatures, which has been observed by various groups<sup>10,46</sup> and for lipids other than DMPC,<sup>10,46,47</sup> is consistent with an expected softening of the bilayers and a decrease in the interbilayer compressibility.<sup>29,46</sup> However, in disagreement with earlier studies,<sup>7,10</sup> we also find a distinct increase in  $\eta_1$  on approaching  $T_M$ . The relatively small increase in  $\eta_1$  may be the reason it was not previously observed by line-shape analysis.<sup>7,10</sup> By definition, line-shape analysis accounts for Bragg peak scattering occurring over a narrow  $q$ -range. Therefore, the small changes in  $\eta_1$  are obscured by the considered limited  $q$ -range. In contrast, the present analysis<sup>23</sup> accounts for the full  $q$ -range including diffuse scattering, thus resulting in better statistics of the Caillé parameter. However, we note that the increase in  $\eta_1$  appears to be much closer to  $T_M$  than the increase in  $d_w$  (Figure 4a). As there are some limitations to our analysis, changes in  $\eta_1$  are only detected when they are pronounced, as in the vicinity of  $T_M$ . Nevertheless, our results are consistent with the presence of increased fluctuations close to  $T_M$ .  $\eta_1$  is inversely proportional to  $d^2$  (eq 3). Since  $d$  is increasing in the vicinity of  $T_M$ , this means that the increase of  $\eta_1$  has to come from a decrease in  $B$  and/or  $K_c$ . At this stage, we are not able to differentiate between the two as  $\eta_1$  contains the product of these two parameters. However, if the high-temperature regime is any indication we would expect a decrease in both  $B$  and  $K_c$ .

Nagle et al.<sup>10</sup> using a Monte Carlo simulation technique predicted a relative increase in  $\eta_1$ , on approaching  $T_M$ , of 35%, if fluctuations would account for the increase in  $d_w$ . This is much larger than the 10% increase observed by us. However, while softening of the bilayer was taken into account (decrease in  $K_c$ ) the same consideration was not given to  $B$ . Nevertheless, the behavior of  $\eta_1$  implies increased bilayer undulations which consequently enhance the steric repulsion of adjacent bilayers,<sup>45</sup> leading to an expansion of  $d_w$  (Figure 4a).

**3.3. Osmotic Pressure Experiments.** To test our contentions from the previous section, we have performed neutron diffraction experiments on oriented multibilayers of DMPC as a function of temperature and osmotic pressure. Osmotic pressure suppresses undulations by bringing bilayers closer together. In other words, if anomalous swelling is due to increased fluctuations, osmotic stress should consequently reduce the amount of swelling. In our case, osmotic pressure,  $P$ , was applied by keeping the sample in direct contact with a solution of PVP. For the temperature range of interest,  $P$  experiences a decrease of between 6% and 8%.<sup>48</sup> Thus, we expect only minor effects from the changes in  $P$  especially in the vicinity of  $T_M$ . Osmotic pressure also increases the main transition temperature, and we observe a maximum of a +1 °C shift in  $T_M$  at  $P = 16$  atm. Results are therefore plotted as a function of  $T - T_M$  (Figure 7).

Figure 7 clearly shows a decrease of the anomalous component of  $d$  with increasing osmotic pressure. On the other hand, Nagle et al.<sup>10</sup> performed similar experiments on multilamellar vesicles of DMPC and DLPC and did not observe any influence of osmotic pressure on the amount of anomalous swelling. This supported their conclusion that fluctuations are not the cause for the expansion of

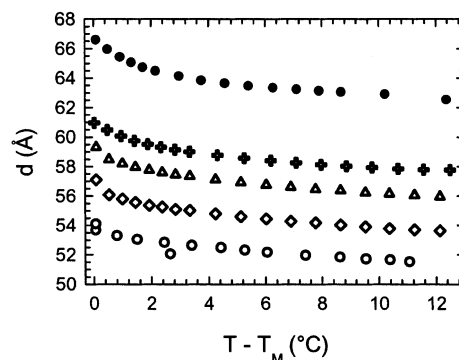


**Figure 7.** Lamellar repeat distance as a function of temperature and osmotic pressures of 0 atm (●), 0.4 atm (+), 2.2 atm (△), 7 atm (◇), and 16 atm (○). The experiments presented here were repeated a minimum of three times for each condition.

the water layer. In contrast, our findings are consistent with fluctuations being the driving force for bilayer repulsion close to  $T_M$  and agree well with the results from the fluctuation parameter analysis (Figure 6). At 16 atm, we find practically no anomalous swelling in  $d$ , which means that the fluctuations have almost entirely been suppressed. Moreover, reduction in swelling upon the application of osmotic pressure is a clear signature of reduced bilayer interactions in the vicinity of  $T_M$ . If this were not the case, the temperature dependence for different osmotic pressures would be similar and would simply be shifted by a constant offset in  $d$ . This point is clearly demonstrated in the temperature range of  $T - T_M > 3$  °C (Figure 7). Thus, the data presented in Figure 7 imply that the  $B$  modulus is reduced and its behavior is analogous to the behavior of  $B$  previously observed in the high-temperature regime of  $L_\alpha$  multibilayers.<sup>29,46</sup>

Why then this decrease in  $B$ ? Following the analysis given above, the only remaining plausible cause is increased steric bilayer repulsion as a result of increased bilayer fluctuations. As shown by Helfrich,<sup>45</sup> the mean square amplitude of the bilayer undulations is inversely proportional to the bending modulus,  $K_c$ , and hence the increase of bilayer undulations has to be attributed to a reduction in  $K_c$ . Using the results from Figures 6 and 7, we thus conclude that in the vicinity of  $T_M$  the bilayers soften, causing them to repel each other and leading to a reduction in  $B$ .

We may visualize this result first, by estimating  $B$  from

$$B \approx -\left(\frac{\partial P}{\partial d}\right)_T \quad (10)$$

for  $P \rightarrow 0$  using the dependence of  $d(T)$  on osmotic pressure (Figure 7). Strictly speaking, this definition gives the thermodynamic  $B$ , which is different from the  $B$  as it appears in eq 3.<sup>33</sup> Quantitative values for  $B$  and  $K_c$  may be obtained from a technique developed in Nagle's lab where the global X-ray diffraction analysis is applied to highly aligned multibilayers.<sup>49</sup> However, we do not expect any changes to the overall trend reported here for  $B$  and  $K_c$ . Their tendency to decrease in the vicinity of  $T_M$  is clearly inferred from Figures 6 and 7. Further, as will become clear later on, the resulting estimates for  $B$  and  $K_c$  compare well with values given in the literature.

The repeat spacings,  $d$ , at a certain temperature and osmotic pressure have been obtained by a smooth spline interpolation of the data presented in Figure 7. Figure 8

(46) Vogel, M.; Münster, C.; Fenzl, W.; Salditt, T. *Phys. Rev. Lett.* **2000**, *84*, 390.

(47) Petrache, H. I.; Tristram-Nagle, S.; Nagle, J. F. *Chem. Phys. Lipids* **1998**, *95*, 83.

(48) Vink, H. *Eur. Polym. J.* **1973**, *7*, 1411.

(49) Lyatskaya, Y.; Liu, Y.; Tristram-Nagle, S.; Katsaras, J.; Nagle, J. F. *Phys. Rev. E.* **2001**, *63*, 011907.

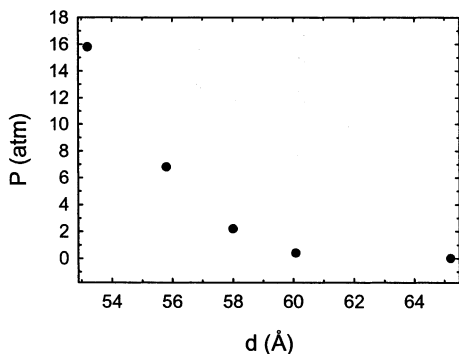


**Figure 8.** Osmotic pressure as a function of lamellar repeat spacing at 25 °C.  $B$  can be estimated from a tangent to the  $P(d)$  curve at each point.

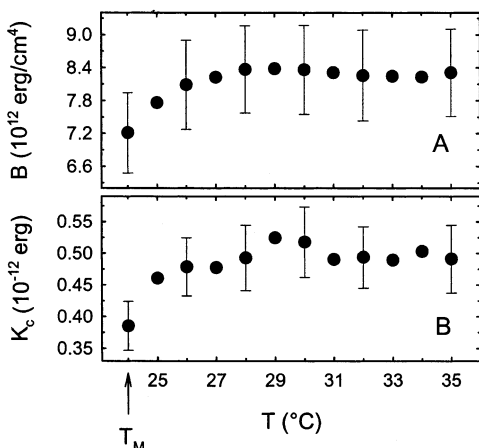


**Figure 9.** Temperature dependence of the compression parameter  $B$  and the bilayer rigidity  $K_c$  in fully hydrated DMPC bilayers. The error for  $B$  and  $K_c$  is on the order of 10%.

shows a typical plot of osmotic pressure versus  $d$ . As expected,  $B$  increases rapidly as the bilayers become more and more compressed. The tangent of the  $P(d)$  plots for  $P \rightarrow 0$  is given in good approximation by the slope of a straight line connecting the data points at 0 and 0.4 atm (Figure 8). The resulting estimates for  $B$  are plotted in Figure 9a. We can then use the estimated  $B$  values and our results of  $\eta_1$  (Figure 6) to calculate the temperature dependence of the bending rigidity by applying eq 3. The results are shown in Figure 9b.

As previously stated, both  $B$  and  $K_c$  experience a distinct drop in the vicinity of  $T_M$ . In the case of  $B$ , we find a constant value of about  $8.3 \times 10^{12}$  erg/cm<sup>4</sup> at temperatures above  $T_M + 4$  °C (Figure 9a), which is reduced by 12% as  $T_M$  is approached.  $B$  has previously not been obtained for fully hydrated DMPC, but our estimate outside the anomalous regime may be compared to a value of  $(6.0 \pm 0.7) \times 10^{12}$  erg/cm<sup>4</sup> for dioleoyl phosphatidylcholine.<sup>49</sup> The bending rigidity, on the other hand, drops from about  $0.48 \times 10^{-12}$  erg at higher temperatures by about 20% in the vicinity of  $T_M$  (Figure 9b). Evans and co-workers report  $K_c = (0.56 \pm 0.06) \times 10^{-12}$  erg for DMPC at 29 °C<sup>50</sup> from micropipet pressurization experiments. The same  $K_c$  has

also been reported from X-ray interaction measurements.<sup>47</sup> Both experimental results agree well with our estimate for  $K_c$ . Nagle et al.<sup>10</sup> arrived at a  $K_c$  value of  $0.4 \times 10^{-12}$  erg close to  $T_M$  from simulations, which also compares well with our estimate (Figure 9b). Fernandez-Puente et al., however, have reported a  $K_c$  about 2 times higher for DMPC.<sup>19</sup> Though, as noted in ref 10, their results may have been biased by constraining the vesicle to have a constant volume.

#### 4. Conclusions

Using a recently developed full  $q$  refinement method,<sup>23</sup> we have analyzed X-ray diffraction data on fully hydrated liposomal dispersions of DMPC in the temperature regime of  $T_M$  to  $T_M + 31$  °C. In terms of structure, we find that anomalous swelling is essentially the result of an expansion of the water layer. The increase in the bilayer thickness is comparable to the increase of  $d$  in DMPE and thus gives no contribution to the observed anomaly. Also, the phosphatidylcholine headgroup does not contribute significantly to the swelling.

A fluctuation parameter analysis revealed that the expansion of  $d_w$  is due to a steric repulsion of bilayers caused by increased fluctuations. Osmotic pressure experiments on highly aligned DMPC multilayers, using neutron diffraction, lend further support to increased fluctuations resulting in an increased  $d_w$ . Moreover, a combination of osmotic pressure studies and fluctuation analysis data led us to the conclusion that the bilayers soften in the vicinity of  $T_M$ , experiencing increased levels of repulsion. To better visualize these results, we have estimated the temperature dependence of  $B$  and  $K_c$ . Results show a 20% drop in  $K_c$  and 12% in  $B$  as  $T_M$  is approached.

Our results are in closest agreement with the work of Mouritsen and co-workers.<sup>6,8</sup> However, their bilayer model only differentiated between a hydrophilic layer, including the headgroup and water layer, and a hydrophobic layer. It was therefore not clear whether there was a contribution from the headgroup. Further, they did not perform a fluctuation analysis but justified their conclusions on the basis of the elasticity measurements by Fernandez-Puente et al.,<sup>19</sup> which, however, have been subjected to some scrutiny in the literature.<sup>10</sup> In contrast, we have been able to arrive at a consistent picture of the structural changes and interactions associated with anomalous swelling through a joint use of X-ray and neutron diffraction data. Finally, we note that it is very likely that the mechanisms described for DMPC bilayers apply also to other systems exhibiting anomalous swelling (e.g., DSPC, DPPC, and DLPC).

**Acknowledgment.** We thank Dmitri P. Kharakoz and Peter Laggner for helpful discussions. G.P. is the recipient of an Erwin Schrödinger Fellowship of the Austrian Science Fund (Grant No. J2004-GEN).

LA026052E

(50) Evans, E.; Rawicz, W. *Phys. Rev. Lett.* **1990**, *64*, 2094. Rawicz, W.; Olbrich, K. C.; McIntosh, T.; Needham, D.; Evans, E. *Biophys. J.* **2000**, *79*, 328.